Contents lists available at ScienceDirect

Current Research in Food Science

Synthesis, characterization and application of antibacterial lactoferrin nanoparticles

Larissa G.R. Duarte , William M.P. Alencar , Raiza Iacuzio , Nathália C.C. Silva , Carolina S. F. Picone [*]

School of Food Engineering, University of Campinas (UNICAMP), 13083-862 Campinas, SP, Brazil

A B S T R A C T

Lactoferrin (L) and gellan gum (G) nanoparticles were produced in different biopolymer proportions through electrostatic complexation to enhance the antimicrobial properties of lactoferrin. The nanoparticles were characterized according to size, charge density, morphology and antimicrobial activity against *S. aureus* and *E. coli,* in two different broths to show the effect of the broth composition on the nanoparticle activity. The 9L:1G particles showed the highest positive zeta potential (+21.20 mV) and reduced diameter (92.03 nm) which resulted in a minimum inhibitory concentration six times smaller (0.3 mg/ml) than pure lactoferrin (2 mg/ml). However, the bacteriostatic action of nanoparticles was inhibited in the presence of divalent cations. When applied to strawberries as a coating, lactoferrin nanoparticles extended fruit shelf-life up to 6 days in the presence of carboxymethylcellulose (CMC). Therefore, lactoferrin-gellan gum complexation was proved to be a promising tool to enhance lactoferrin antimicrobial action and broaden its application as a food preserver.

1. Introduction

Currently, there is an increasing consumer demand for healthier, natural foods without chemical additives. This highlights the need for alternative solutions to traditional synthetic antimicrobials, such as the use of antimicrobial proteins as biopreservers (Tkaczewska, 2020).

Milk proteins have been studied in this sense due to their technological and functional properties, and they are recognized as safe (GRAS). In addition to being a valuable source of bioactive peptides, these proteins can also act as texture modifiers and emulsifiers (Saraiva et al., 2017). Lactoferrin is a globular glycoprotein present in milk, mainly in colostrum with recognized antimicrobial activity (Gonzalez-Chavez et al., 2009). It has a molecular weight of 80 kDa and an isoelectric point (pI) of 8. Its structure is formed by two symmetrical lobes (lobes N and C) which show high affinity to Fe^{+2}, Cu^{+2}, Zn^{+2} and Mn^{+2} binding (McCarthy et al., 2014; Iglesias-Figueroa et al., 2019).

Lactoferrin antimicrobial activity is related to its ability to sequester iron and cause a shortage of essential nutrients for microorganism Lactoferrin antimicrobial activity is related to its ability to sequester iron and cause a shortage of essential nutrients for microorganism growth. In gram-negative bacteria, lactoferrin binds to the lipid A portion of lipopolysaccharide (LPS) present in the outer cell membrane and releases

LPS from the cell wall (Kanwar et al., 2015; Iglesias-Figueroa et al., 2019). In gram-positive bacteria, lactoferrin binds to phosphate groups (negative charges) of lipoteichoic acid present on the wall of the cell and damages the outer membrane of the bacteria (Tomita et al., 2006; Ibrahim Al-Mashahedah et al., 2019). Different strategies have been used to increase lactoferrin antimicrobial activity, such as enzymatic hydrolysis (Elbarbary et al., 2010; Quintieri et al., 2012), chemical modification (Nakamura, 2002; Pan et al., 2007) and physical treatments such as high pressure homogenization (Iucci et al., 2007). Lactoferrin properties can also be enhanced by nanoaggregation. The antimicrobial potential of polymers has been recently reported to rise when compounds are added to nanoparticles. Nanoaggregation can result in a better distribution of cationic charges on the polymer surface and thus, enhance interactions with anionic microbial membranes (Lam et al., 2018).

Many techniques have been reported for the production of protein nanoparticles, such as: thermal gelation (Bengoechea et al., 2011; Bourbon et al., 2016), layer-by-layer deposition (Liu et al., 2017), nano spray drying (Bourbon et al., 2019), simple antisolvent precipitation methods (Chen et al., 2020), solvent displacement (Oliveira et al., 2016), coprecipitation (Zhang et al., 2019), ionotropic gelation (Tammam et al., 2018), and emulsification methods (Kumar et al., 2017;

Sabra and Agwa, 2020). However, many of these procedures involve the use of base or strong acids, high temperatures or large amounts of salts, which can cause protein denaturation and consequently alter its functional properties such as antibacterial activity (Franco et al., 2018).

Electrostatic complexation is based on the use of two oppositely charged molecules, as positively charged proteins and negatively charged polysaccharides, due to the electrostatic interactions established at pH values below the pI of proteins (Babaei et al., 2019).

The nature of the complexes formed depends on the type and concentration of the polysaccharide chosen, pH, ionic strength and temperature (Bokkhim et al., 2015; Gulão et al., 2014). Bengoechea et al. (2011) studied the interaction of lactoferrin with pectin at pH 7 and found that increasing the concentration of pectin resulted in negatively charged complexes. Peinado et al. (2010) prepared lactoferrin complexes with three different polysaccharides and showed that the type and concentration of polysaccharide and the medium pH and ionic strength were important parameters for the formation and stability of the complexes. Lactoferrin-pectin complexes proved to be more stable than lactoferrin-carrageenan and lactoferrin-alginate complexes.

Gellan gum is a nontoxic and biodegradable polysaccharide, produced by *Sphingomonas elodea*, with intense gelation capacity even at low concentrations (Torres et al., 2019; Mirón-Mérida et al., 2019; Xu et al., 2019; Picone and Cunha, 2013). It has an anionic character (pKa of 3.5) due to the presence of glucuronic acid (de Jong and van de Velde, 2007) on its structure, and has outstanding potential for interaction with lactoferrin. Although the interaction between these biopolymers has been previously reported in the literature (Bastos et al., 2019; Ueno et al., 2012), the antimicrobial properties of lactoferrin-gellan complexes were still unexplored and the application of such complexes in real food is scarce. Despite this, the electrostatic interaction between gellan gum and lactoferrin seems to be a promising strategy to increase lactoferrin antimicrobial properties without the aid of inorganic compounds and thus, enlarge its use as a food preserver.

The aim of this work was to produce lactoferrin nanoparticles through electrostatic complexation to gellan gum to increase its antimicrobial capacity without the aid of inorganic compounds and expand its use as a natural preservative of food products. The interactions between the compounds were evaluated by infrared spectroscopy (FTIR) and isothermal titration calorimetry (ITC). Different proportions of biopolymers were assessed to model the size, zeta potential and morphology of nanoparticles to understand how these properties influence the antimicrobial functionality of the samples. The antimicrobial action was evaluated by *in vitro* assays against *S. aureus* and *E. coli*. The effect of the environment on the antimicrobial properties of nanoparticles was also analyzed by the use of two different culture broths. Finally, the nanoparticles were applied to coat strawberries in order to prolong their preservation.

2. Materials

The materials used for the synthesis of the nanoparticles were lyophilized bovine lactoferrin with a purity of 96% (w/w) supplied by Bega Bionutrients (Tatura, Australia), deacylated gellan gum (Kelcogel® F) (3.42% w/w of moisture and with 9.3% (w/w) of ash) kindly donated by Kelco Biopolymers (San Diego, CA), Triptona Soy broth – TSB (Kasvi), GYP broth composed of glucose (Dinâmica), peptone and yeast extract (Acumedia), Brain and Heart Infusion broth – BHI (Kasvi) and bacterial agar (Kasvi). Carboxymethylcellulose (CMC) was acquired from Dinâmica (Indaiatuba, SP), and fresh San Andreas organic strawberries were obtained shortly after harvesting from a local producer (Paulinia, Brazil). All other reagents were of analytical grade.

3. Methods

3.1. Synthesis and characterization of nanoparticles

3.1.1. Preparation of stock solutions

The gellan gum stock solution (0.1%, w/v) was prepared by powder dissolution in ultrapure water (Milli-Q, Millipore) under magnetic stirring at 80°C for 30 min in a jacketed beaker connected to a thermostatic bath. After that, the solution was cooled in an ice bath to 25°C. Lactoferrin stock solution (0.1%, w/v) was prepared by powder dissolution in ultrapure water under magnetic stirring at room temperature for 1 h at 300 rpm.

3.1.2. Production of nanoparticles

First, pH scans were carried out to assess the zeta potential variation of lactoferrin and gellan gum and thus, to determine the ideal pH for the formation of nanoparticles. The pH of lactoferrin and gellan solutions was adjusted from 3.5 to 8.5 with NaOH or HCl (1 mol. L^{-1}) and their zeta potential and size were recorded by dynamic light scattering (DLS) according to section 3.3. At pH 4, the most intense net charge difference between biopolymers was observed; therefore, it was chosen to form nanoparticles. With this aim, the stock solutions were vacuum filtered and mixed in different proportions (Table 1) using a rotor-stator (Ultra Turrax, IKA T25) at 10,000 rpm for 3 min at 25°C. The final concentration of biopolymers in the samples was kept constant at 0.1% (w/v).

For antimicrobial tests and FTIR analysis, the nanoparticles were previously lyophilized for 48 h at -55 °C and 98 μmHg.

3.1.3. Dynamic Light Scattering (DLS)

The zeta potential of biopolymers and nanoparticles was measured in a ZetaSizer Nano-ZS (Malvern Instruments, Worcestershire, United Kingdom) operated with a He–Ne laser (633 nm). The intensity of the scattered light was measured at 173° by a photodiode. The hydrodynamic diameter of the biopolymers and nanoparticles was evaluated in triplicate using the same equipment. Size and zeta potential values were expressed as the mean ± standard deviation. For the size results, the number distribution was used. All the samples showed monomodal distributions.

3.1.4. Isothermal Titration Calorimetry (ITC)

The titrations were performed in triplicate using a VP-ITC MicroCalorimeter, available from the Brazilian Biosciences National Laboratory (CNPEM). The test was performed to determine the main thermodynamic parameters associated with the formation of nanoparticles, such as reaction enthalpy, Gibbs free energy and entropy (Xiong et al., 2016). The following parameters were used: 45 injections of 10 μL each, response time of 250 s, stirring speed of 307 rpm, cell temperature equal to 25 °C, initial delay of 120 s and spacing time of 250 s. Lactoferrin (10.4003 μmol L^{-1}) was placed in the syringe, and gellan (1.000 μmol L^{-1}) was placed in the cell. Two blanks that reproduced the adopted system were performed, the first one with lactoferrin in the syringe and Milli-Q water allocated in the cell, and the second one with Milli-Q water in the syringe and gellan gum in the cell. Before placing the samples in the syringe and the cell, they were deaerated under vacuum for 5 min. The experiments were conducted at 25°C, and

Table 1
Composition of lactoferrin-gellan nanoparticles.

Nanoparticles	Gellan (% w/v)	Lactoferrin (% w/v)
2L: 8G	0.080	0.020
5L: 5G	0.050	0.050
6L: 4G	0.040	0.060
7L: 3G	0.030	0.070
8L: 2G	0.020	0.080
9L: 1G	0.010	0.090

the data were analyzed using *Origin* software. All solutions were evaluated at pH 4. The heat of dilution of lactoferrin was measured by titration in Milli-Q water and subtracted from the raw data.

3.1.5. FTIR analysis

The spectra were obtained using an FTIR spectrophotometer, model IRPrestige-21, manufacturer Shimadzu (Kyoto, Japan). Two milligrams of each compound (lactoferrin, gellan gum or nanoparticles) was filled with KBr (200 mg), and then the mixtures (KBr + compounds) were compressed at 80 kN for 10 min under vacuum in 13 mm diameter tablets.

The spectra were read in the 4000- 400 cm^{-1} range with a resolution of 4 cm^{-1} for all treatments.

3.1.6. Atomic Force Microscopy Analysis (AFM)

The size and morphology of the particles were evaluated by atomic force microscopy in a Park NX-10 microscope from the National Laboratory of Nanotechnology (LNano) of CNPEM. The nanoparticles were diluted 3 times prior to observation.

One drop of each diluted solution was deposited on mica and dried under gaseous nitrogen. After drying, the samples were examined under the microscope to collect images which were treated in *Gwyddion* 2.54 software. At least five measurements of each sample were carried out to obtain their mean diameter.

3.1.7. Antimicrobial activity of nanoparticles

To assess the antimicrobial capacity of the nanoparticles, minimum inhibitory concentration (MIC) assays were performed against *S. aureus* (gram positive) and *E. coli* (gram negative) isolated from a Minas cheese factory environment. The microorganisms were provided by the Laboratory of Food Microbiology II of the Department of Food Science and Nutrition, University of Campinas (Brazil) and were confirmed by PCR.

The minimum inhibitory concentration was taken as the lowest concentration of nanoparticles that caused complete inhibition of bacterial growth (Bellamy et al., 1992). The tests were performed in triplicate. This analysis was determined by the microdilution method in sterile 96-well microplates containing tryptic soy broth (TSB) or GYP (glucose, peptone and yeast extract) culture medium. The bacterial cultures were grown in BHI broth, incubated for 24 h at 37 °C and their concentration was adjusted to 10^3 CFU/mL. Then, 96-well flat-bottom plates were filled with different broths, microorganisms and different concentrations of samples and incubated at 37 °C for 24 h. After 24 h, 50 μL of 0.01% (w/v) resazurin dye was applied to each well of the plate. The change in color from blue to pink was considered an indicator of microbial growth. Control wells were prepared using pure broth, nanoparticle solutions and pure cultures to avoid false positive and false negative results.

In the tests of minimum bactericidal concentration (MBC), 10 μL of the well of minimum inhibitory concentration and three higher concentrations from the MIC analysis were inoculated in a petri dish with nutrient agar. The plates were incubated for 24 h at 37 °C. The growth of cultures indicates that the nanoparticles had bacteriostatic effects; that is, they inhibited microbial growth but did not eliminate it completely. The absence of bacterial growth indicates that the samples are bactericidal; that is, it induces the death of up to 99.99% of the microorganisms (Fernández, 2015).

3.2. Analysis of minerals in microbiological broths

The minerals iron, zinc, copper and manganese were quantified in TSB and GYP broths.

The samples were digested with concentrated nitric acid in two stages, first in the digestion block, for 24 h at 110 °C, and second for 2 h at 130 °C. The extracts were diluted with ultrapure water and inserted into a flame atomic absorption spectrophotometer (PerkinElmer AAnalyst 200 Atomic Absorption Spectrometer, Waltham, USA). The analyses

were performed in triplicate.

3.3. Preparation of the strawberry coating solution

Strawberries were disinfected by immersion in NaClO 0.02% (v/v) solution for 15 min, followed by immersion in the coating solution for 2 min and drying in a laminar flow chamber (Pachane, Brazil) previously UV-sterilized for 1 h. Two compositions of the coating solution were evaluated (Table 2): solutions of pure nanoparticles (NP) and nanoparticles plus carboxymethylcellulose (NP + CMC) (to improve nanoparticle adherence to the fruit surface). Moreover, part of the fruits was coated only by CMC and the other group was not coated (control). Each group was stored at 25 °C and 50% relative humidity for six days.

3.4. Determination of fruit quality

3.4.1. Weight loss

The strawberries were weighed before coating, after two (48 h) and 6 days of storage (144 h) at 25°C and 50% UR. The cumulative weight loss during storage in relation to the initial weight was calculated and expressed as a percentage.

3.4.2. Titratable Acidity (TA)

The methodology of Gao et al. (2020) was followed. Ten grams of strawberries was crushed in 100 mL of ultrapure and filtered water. Two drops of 1% (w/v) phenolphthalein were added to 20 mL of extract, followed by titration with 0.1 mol/L NaOH. The titratable acidity (TA) was calculated using Eq. (1).

$$TA_{content} = \frac{V_{NaOH} \times V_e \times c \times K_c}{V_S \times m} \times 100\% \tag{1}$$

where V_{NaOH} is the volume of NaOH solution consumed during the titration (mL); V_e is the total volume of the strawberry extract (mL); c is the molar concentration of the NaOH solution (mol/L); Kc is the milliequivalent citric acid factor, 0.064 g/mmol; V_s is the volume of strawberry extract used for titration (mL); and m is the total strawberry mass used to prepare the pulp (g).

3.4.3. Content of total soluble solids (TSS) and pH

The content of soluble solids and pH of strawberries were determined in a refractometer (Kasvi, Brazil) and pH meter (Gehaka PG2000, Brazil), respectively. Both analyses were performed in fresh strawberries after 24 and 144 h of storage at 25°C and 50% UR.

3.4.4. Total aerobic mesophilic bacteria counts

The determination of aerobic mesophilic bacteria was performed by a pour plate on plate count agar in fresh strawberries after 24 and 144 h of storage at 25°C and 50% UR. The strawberries were crushed and 25 mL of the pulp from each group was diluted and homogenized in 225 mL of sterile 0.1% peptone water. Serial dilutions were made in triplicate with sterile 0.1% peptone water. One milliliter of each dilution was distributed in empty and sterilized Petri dishes. Then, 15 to 20 mL of plate count agar (PCA) culture medium previously cooled to 45 °C was

Table 2
Composition of strawberries coating solutions.

Treatments	Nanoparticle concentration 9L:1G (%w/v)	Concentration CMC (%w/v)
Control	–	–
CMC	–	0.5
NP	0.003	–
NP + CMC	0.003	0.5

Control: uncoated strawberries, CMC: strawberries coated with carboxymethylcellulose, NP: strawberries coated with nanoparticles, NP + CMC: strawberries coated with nanoparticles and carboxymethylcellulose.

added to the plates, and mixed. After complete solidification of the culture medium, the plates were inverted and incubated at 37 °C for 48 h. The plates with minimum and maximum limits of 25 and 250 colonies were selected to measure the number of mesophilic microorganisms per volume of the sample (CFU/ml) (Sogvar et al., 2016b).

3.5. Statistical analysis

Differences between means were evaluated using *Sisvar* software (Ferreira, 2019). Analysis of variance (ANOVA) was carried out and the Tukey test at the level of 5% of significance was applied to evaluate the differences between means.

4. Results and discussions

4.1. Characterization of nanoparticles

4.1.1. Study of biopolymer zeta potentials

Fig. 1 shows that the zeta potential of lactoferrin varied from +27.3 to -2.59 mV within the pH range evaluated (3.5 to 8.5). The lactoferrin isoelectric point was observed at pH 8, where the zeta potential changed from positive (at low pH values) to negative. The cationic character of lactoferrin at pH values lower than 8.0 is related to the presence of the positive amino acids lysine and arginine in its structure (Moore et al., 1997). Lactoferrin has 700 amino acids, mostly basic divided into two symmetrical lobes N and C, both carrying an iron binding site (Bourbon et al., 2019). Due to its cationic characteristics and the ability to sequester iron, lactoferrin has biological activities such as antibacterial and antifungal action (Franco et al., 2018).

The zeta potential of gellan gum ranged from -25.1 to -33.1 mV. Gellan has a pKa of 3.5, and its anionic character is related to the presence of glucuronic acid on the gellan gum structure (de Jong and van de Velde, 2007). At pH values higher than the polysaccharide pKa, the carboxylic groups dissociate from glucuronic acids (Horinaka et al., 2004) resulting in a negative zeta potential.

To form nanoparticles by electrostatic complexation, both compounds must have opposite charges. Picone and Cunha (2013) formed nanoparticles of chitosan and gellan gum by electrostatic complexation and observed that at pH 4.5 there was a greater difference in zeta potential between these compounds. Regarding the zeta potentials of

lactoferrin and gellan gum at different pH values (Fig. 1), the ideal pH for lactoferrin-gellan gum complexation is 4.0, since at this pH, there is a greater variation in charges across the compounds.

4.1.2. Physico-chemical properties of nanoparticles

The zeta potential and the size of nanoparticles composed of 6 different proportions of lactoferrin-gellan gum are shown in Table 3.

At pH 4.0, pure gellan gum showed a negative charge (-35.70 mV, Table 3), close to the values found by Fasolin et al. (2013) between pH 3.0 and 4.0, (from -25 mV to -40 mV), respectively. The nanoparticles 2L:8G and 5L:5G also showed negative zeta potential (-31.27 and -30.30 mV, respectively), as they contain a considerable proportion of gellan gum compared to the lactoferrin concentration. Despite the higher proportion of lactoferrin compared to gellan gum, nanoparticles 6L:4G and 7L:3G showed negative zeta potential (-27.27 and -26.40 mV, respectively) but with a lower negative charge density compared to nanoparticles 2L:8G and 5L:5G.

As the amount of lactoferrin increases in nanoparticles, there is an increase in their positive charge. Nanoparticles 8L:2G and 9L:1G showed increasing zeta potentials (+8.93 and + 21.20 mV, respectively) up to pure lactoferrin solutions (+33.70 mV). Moore et al. (1997) studied the structure of lactoferrin and found that the positive charge is concentrated in the lower left part, or in the N lobe of the compound, due to the large amount of positive amino acids lysine and arginine in this region.

Table 3

Zeta potential and hydrodynamic diameter of pure gellan gum (G) solution, pure lactoferrin (L) solution and nanoparticles composed of different proportions of lactoferrin and gellan gum.

Sample	Zeta Potential (mV)	Hydrodynamic diameter (nm)
Pure gellan gum	−35.70 ± 1.54[a]	22.11 ± 1.04[a]
2L:8G	−31.27 ± 0.29[a]	59.93 ± 27.92[a]
5L:5G	−30.30 ± 0.10[b]	85.37 ± 24.15[a]
6L:4G	−27.27 ± 1.87[b]	82.00 ± 13.11[a]
7L:3G	−26.40 ± 3.73[c]	73.60 ± 20.79[a]
8L:2G	+8.93 ± 1.23[d]	217.33 ± 65.24[b]
9L:1G	+21.20 ± 1.25[e]	92.03 ± 13.61[a]
Pure lactoferrin	+33.70 ± 0.66[f]	3.81 ± 0.33[ac]

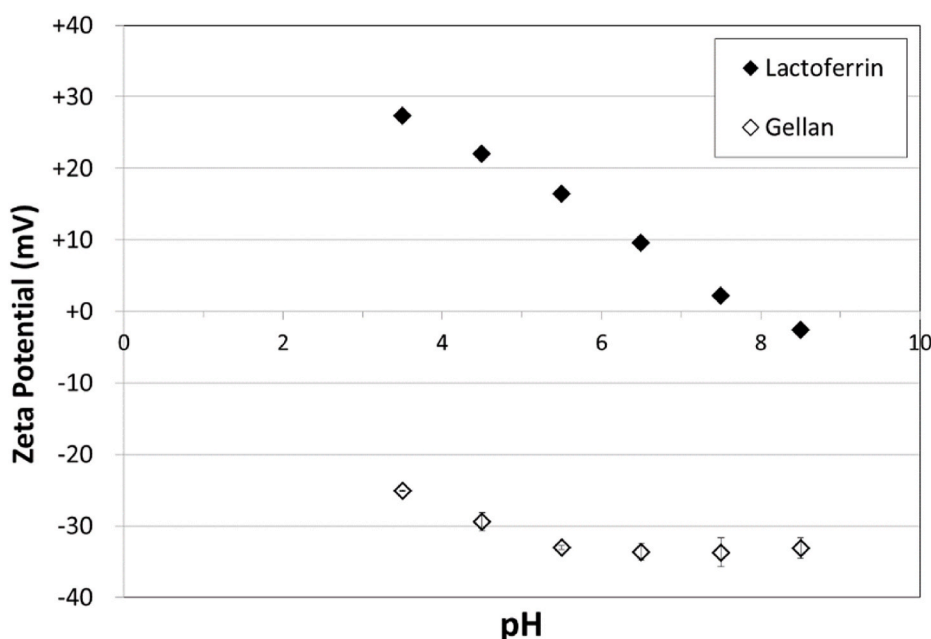Different letters in the same column indicate significant differences between means (p-value < 0.05).

Fig. 1. Zeta potential of gellan gum and lactoferrin solutions at different pH values.

The complexes showed monomodal size distributions (considering the number distribution). The diameter of pure gellan gum was 22.11 nm and was in agreement with the work of Grasdalen and Smidsrød (1987), who reported sizes between 20 and 100 nm for the same polysaccharide. The sizes of nanoparticles 2L:8G, 5L:5G, 6L:4G and 7L:3G were similar, with no significant difference (59.93, 85.37, 82.00 and 73.60 nm, respectively). With the increase in the proportion of gellan gum, there is an excess of negative charge so that repulsive interactions prevail, favoring the formation of small particles.

Nanoparticles 8L: 2G were the ones with the largest size (217.33 nm) because of their low zeta potential (+8.93 mV). Close to neutrality, there is a balance between positive and negative charges, which causes the aggregation of particles due to the absence of repulsive interactions (Picone and Cunha, 2013).

Nanoparticles 9L:1G presented the highest zeta potential of all nanoparticles (Table 3), suggesting that the amount of gellan gum was not sufficient to neutralize all the lactoferrin amino groups of this sample. This high positive zeta potential indicates a possible antimicrobial functionality, which is usually related to the cationic character of lactoferrin. The size of these nanoparticles (92.03 nm) results from the high density of positive charges that induce electrostatic repulsion between particles and thus the formation of nanoparticles smaller than 100 nm and with low polydispersity.

The gellan gum is formed by parallel double helices stabilized by hydrogen bonds between the chains of its carboxyl groups (Chandrasekaran et al., 1988; Cassanelli et al., 2019). When deacylated, the gellan gum structure extends and acquires a greater length than the original one (O'Neill et al., 1983). The molecular weight (1640 kDa) of gellan gum is higher than that of lactoferrin (80 kDa), as well as the hydrodynamic diameter values observed in the present study (Table 3) (Sworn and Kasapis, 1998; Baker and Baker, 2005; Padrão et al., 2020). Therefore, because it is smaller than gellan gum and has greater flexibility, lactoferrin molecules mold to the polysaccharide structure (EL-Fakharany, 2020) and thus a higher concentration of the protein is necessary to fully neutralize the gellan gum anionic sites.

4.1.3. Isothermal titration calorimetry (ITC)

ITC is a useful technique to measure the thermodynamic parameters involved in the complexation of proteins and polysaccharides (Zheng et al., 2020; Yang et al., 2020). In this work, ITC was used to investigate the molecular interaction between lactoferrin and gellan gum at pH 4.0 and 25 °C. From the resulting titration curve between lactoferrin and gellan gum, the enthalpy change ΔH, the binding constant (K) and stoichiometry (n) of biopolymer complexation were acquired (Fig. 2, Table 4). The Gibbs free energy (ΔG) and entropy variation (ΔS) of the reaction were also calculated using the relationship ΔG = ΔH – TΔS (Zheng et al., 2020; Su and Xu, 2018; Yang et al., 2020). Fig. 2 shows the ITC thermogram of the heat flow as a function of time (A) and the lactoferrin/gellan gum binding isotherm (B) obtained by the integral of the titration peaks and subtracted from the dilution values (control).

It is worth noting that the peak areas gradually decrease due to the reduction of free gellan gum until they reach a stable equilibrium state, indicating the saturation point of lactoferrin-gellan gum interaction. Saturation was achieved after 24 injections of 10 μL each. The thermodynamic parameters of enthalpy, entropy, binding constant and association were determined using the one-site model (Wang et al., 2019) (Table 4).

The stoichiometry or the *n*-value for the lactoferrin-gellan gum system was 0.745, which represents the number of identical and independent binding sites for lactoferrin in the gellan gum and indicates the strength of the association considering the 1-site interaction model (Wang et al., 2019).

Gibbs' enthalpy, entropy and free energy showed negative values, indicating that the complexation processes were dominated by the change in enthalpy (Wang et al., 2019; Xiong et al., 2017). The negative ΔH value (Table 4) reveals an exothermic reaction and indicates that
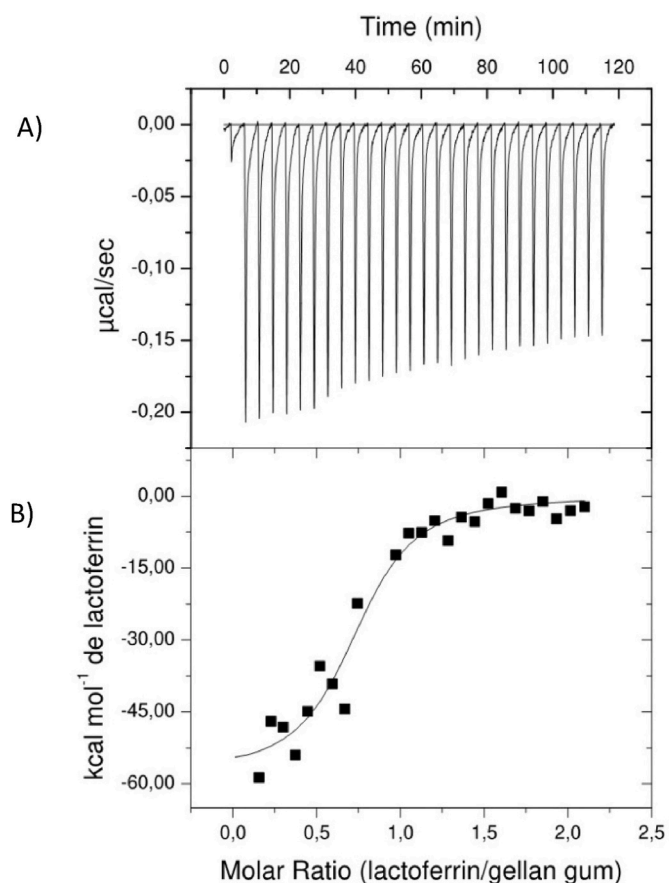

Fig. 2. A) Heat flow curve versus time and B) isothermal binding of lactoferrin (L) titrated in gellan gum (G) according to the L/G molar ratio.

Table 4

Thermodynamic parameters of the lactoferrin-gellan interaction.

	ΔH (KJ/mol)	ΔS (KJ/mol.K)	ΔG (KJ/mol)
Lactoferrin-gellan gum	−312.42 ± 8.37	−0.817 ± 0.13	−68.74 ± 4.81

ΔH = enthalpy, ΔS = entropy, ΔG = Gibbs free energy.

complexation was energetically favorable and occurred due to the establishment of electrostatic interactions or hydrogen bonds (Wang et al., 2019; Zheng et al., 2020). The negative ΔH and ΔS values and the absolute ΔH value being higher than the absolute ΔS value indicate that, in addition to electrostatic interactions, hydrogen bonds and van der Waals forces influenced lactoferrin-gellan gum complexation (Yang et al., 2020). Two processes can dominate the interaction between proteins in the formation of nanoparticles (Xia et al., 2020). One of them is exothermic and involves noncovalent complexation (electrostatic forces, van der Waals attraction and hydrogen bonds) and the other one is endothermic with reorganization and release of interfacial water. When proteins are more hydrophobic, the process is usually endothermic since hydrophobic interactions need energy to break hydrogen bonds (Zheng et al., 2020).

The formation of protein-polysaccharide complexes is spontaneous when the Gibbs free energy of the system is negative (Schmitt et al., 1998; Turgeon and Laneuville, 2009). In this study, ΔG was -68.74 kJ/mol, which indicates the spontaneous character of electrostatic complexation.

The high value of the association constant K, 2.22×10^7, confirms the intense interaction between the compounds, which can be attributed to the high charge density of gellan gum (-35.70 mV) and lactoferrin (+33.70 mV) (Wang et al., 2019).

4.1.4. Fourier transform infrared spectroscopy (FTIR)

The intermolecular interactions between the lactoferrin protein and gellan gum were analyzed by FTIR (Fig. 3).

In the lactoferrin spectrum, the peaks at 2993 cm^{-1} and 2887 cm^{-1} correspond to the C–H stretching vibration indicating the presence of one or more alkane groups. The 1592 cm^{-1} peak corresponds to the C=C stretching vibration of aromatic rings present in aromatic amino acids such as tryptophan. The 1417 cm^{-1} peak corresponds to the angular deformation vibrations of C–H. The peaks at 1344 cm^{-1} and 1184 cm^{-1} refer to the stretching of N–H (Holler et al., 2009).

In the spectrum of gellan gum, the peak at 3003 cm^{-1} corresponds to the elongation of –OH, and the peak at 1541 cm^{-1} corresponds to the C–O stretching of glucuronic acid (Agibayeva et al., 2020). The peak at 1592 cm^{-1} is present in the spectrum of lactoferrin and nanoparticles, similar to the peak at 3003 cm^{-1}, which is present in the spectrum of nanoparticles and gellan gum, confirming that these two compounds were present in nanoparticles.

In the spectrum of nanoparticles, peaks at 2947 cm^{-1} and 2887 cm^{-1} refer to stretching of C–H and peaks at 1344 cm^{-1}, 1290 cm^{-1} and 1190 cm^{-1} correspond to stretching of C–N.

In the region between 1500 and 900 cm^{-1}, there are several peaks in the spectrum of nanoparticles. Amide II can be associated with the peak at 1476 cm^{-1}, which refers to the angular deformation of N–H and C–N stretching. Peaks from 1423 to 1290 cm^{-1} correspond to C–N stretching and N–H angular deformation, and are associated with amide III (Santos et al., 2018). The peak at 1480 cm^{-1} present in the lactoferrin spectrum shifted to 1476 cm^{-1} in the nanoparticle spectrum indicating that the compounds are interacting by electrostatic interactions (Yang et al., 2019; Duca et al., 2018).

4.1.5. Atomic Force Microscopy (AFM)

The morphology and size of the 9L:1G nanoparticles were evaluated by atomic force microscopy (Fig. 4), as they showed promising zeta potential and size values for antimicrobial functionality.

AFM images revealed small nanoparticles 16.33 ± 1.52 nm in diameter, differing from the sizes found by DLS analysis (92.03 ± 13.61 nm) (Table 3). This variation in size was expected due to the principle of the different techniques (DLS and AFM) used. In DLS analysis, dynamic light scattering is correlated with the hydrodynamic radius of the
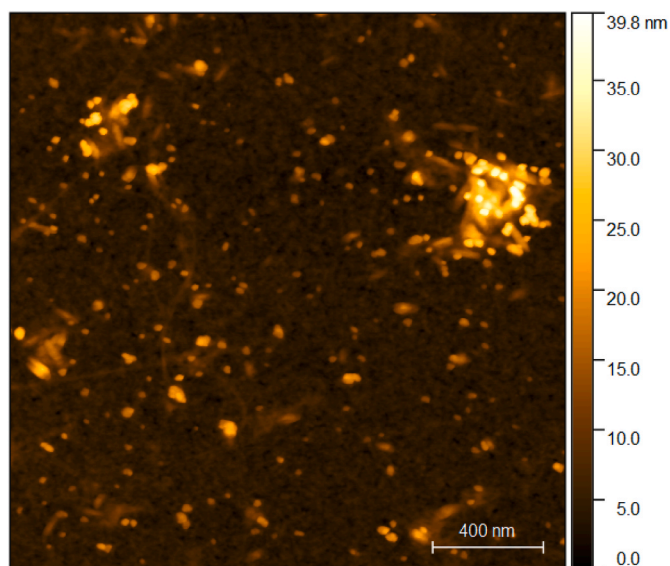

Fig. 4. Morphology of 9L:1G lactoferrin-gellan nanoparticles visualized by atomic force microscopy.

nanoparticles considering their respective solvation layer, so the size values are usually higher than those obtained by microscopy (Holler et al., 2009; Bollimpelli et al., 2016). In addition, the prior preparation of the samples in the different techniques must also be considered. In the AFM technique, nanoparticles are placed on a mica surface and dried in gaseous nitrogen before analysis on the microscope, which can result in partial shrinkage of the samples (Ribas Fonseca et al., 2020).

4.1.6. Antimicrobial properties of nanoparticles

Table 5 shows the results of the minimum inhibitory concentration of lactoferrin and lactoferrin-gellan gum nanoparticles in different broths (GYP and BHI) against the microorganisms *E. coli* and *S. aureus*.

To present antimicrobial functionality, the nanoparticle should be positively charged to interact with the anionic sites of the bacterium and thus cause the membrane rupture. This theory is confirmed in this study
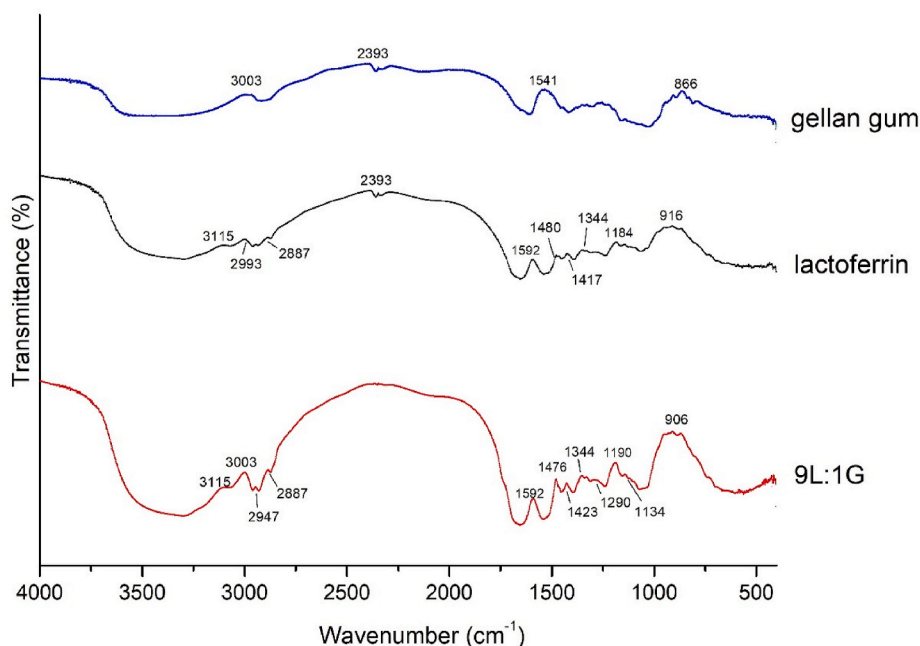

Fig. 3. Spectra of lactoferrin, gellan and lactoferrin-gellan nanoparticles (9L:1G).

Table 5

Minimum inhibitory concentration (MIC) of lactoferrin and nanoparticles in two different broths: TSB (tryptic soy broth) and GYP (glucose, peptone and yeast extract).

Compound	Broth	Microorganism	MIC (mg/ml)	MBC
Lactoferrin	TSB	*E. coli*	a	b
Lactoferrin	GYP	*E. coli*	a	b
Lactoferrin	TSB	*S. aureus*	4.0[a]	b
Lactoferrin	GYP	*S. aureus*	2.0[ab]	b
Nanoparticles 9L:1G	TSB	*E. coli*	a	b
Nanoparticles 9L:1G	GYP	*E. coli*	a	b
Nanoparticles 9L: 1G	TSB	*S. aureus*	a	b
Nanoparticles 9L: 1G	GYP	*S. aureus*	0.3[b]	b
Nanoparticles 2L:8G	TSB	*E. coli*	a	b
Nanoparticles 2L:8G	GYP	*E. coli*	a	b
Nanoparticles 2L:8G	TSB	*S. aureus*	a	b
Nanoparticles 2L:8G	GYP	*S. aureus*	a	b

Means followed by different letters in the same column differ significantly from each other at the 5% level of significance.

[a] Showed no inhibition at concentrations up to 8 mg/ml.

[b] Showed no bactericidal action.

by the effectiveness of 9L:1G positive nanoparticles in comparison to 2L:8G negative nanoparticles, which did not show any inhibitory effects (Table 5). The nanoparticles of lactoferrin-gellan gum 9L:1G had +21.20 mV zeta potential, while the 2L:8G had -31.27 mV (Table 3).

Table 5 shows a greater antimicrobial efficacy of 9L:1G nanoparticles (0.3 mg/ml) in GYP broth against *S. aureus* when compared to pure lactoferrin (2.0 mg/ml). This improvement is possibly related to a better distribution of positive charges on the nanoparticle surface and changes on its surface amphipathic balance after nanoaggregation (Ren et al., 2017; Lam et al., 2018). Alpha helices are predominant in the secondary structure of lactoferrin and are related to amphiphilic domains of protein structure. It presents patches of hydrophobic residues on one face with tryptophan side chains. On the opposite face, the presence of charged amino acid side chains (such as arginine) confers hydrophilic domains to the structure (Vieira et al., 2021; Vega Chaparro et al., 2018). This amphiphilic character of the lactoferrin structure facilitates its interaction with microorganisms. Initially the positively charged residues of lactoferrin interact electrostatically and through multiple hydrogen bonds with the negatively charged surface of bacteria. Then, their hydrophobic residues anchor in the lipophilic portion of the microorganism membrane and release lipopolysaccharide from the bacterial membrane (Haney et al., 2007; Wang et al., 2021).

The MIC against *S. aureus* of lactoferrin and its nanoparticles (Table 5) were lower than other values reported in the literature. Shahidi et al. (2020) evaluated lactoferrin antimicrobial activity against *Staphylococcus aureus* PTCC1337 and found MIC at 8 mg/mL of bovine lactoferrin. The differences in inhibitory action observed in relation to the pure lactoferrin sample of the present study are probably related to the different broths and strains evaluated. Regarding *E. coli*, the samples were not capable of inhibiting microorganism growth in the concentration range evaluated (Table 5). The presence of antimicrobial activity against *S. aureus* and the absence against *E. coli* is also related to the difference in the chemical complexity of the cell walls of these gram-positive and gram-negative microorganisms, respectively. The outer membrane that lines the peptidoglycan cell wall of gram-negative bacteria makes them less sensitive to some antimicrobials (Seibert et al., 2019; Barreiras et al., 2020).

In addition to the type of microorganism, the broth used for growth also interfered with nanoparticles' antimicrobial action, evidencing the influence of the environment on the interaction and action mechanisms of the nanoparticles. In GYP broth (1% peptone, 0.025% yeast extract and 1% glucose), the lactoferrin-gellan gum nanoparticles showed a minimum inhibition concentration against *S. aureus* of 0.3 mg/ml, but showed no inhibition in TSB broth. The high concentration of divalent cations Fe^{2+}, Mn^{2+}, Zn^{2+} and Cu^{2+} present in TSB broth (Table 6) causes

Table 6

Quantity of iron, zinc, copper and manganese minerals present in GYP and TSB broths.

Broth	Iron (mg/kg)	Zinc (mg/kg)	Copper (mg/kg)	Manganese (mg/kg)
GYP	<1.50	<0.12	<0.40	<0.15
TSB	9.45 ± 0.77	33.61 ± 1.16	1.08 ± 0.02	1.10 ± 0.02

salts to compete for the anionic sites of the microbial membrane, decreasing the capacity of lactoferrin to destabilize the bacterial cell wall. This was confirmed by the higher MIC value observed for pure lactoferrin in TSB broth (4.0 mg/ml) compared to the MIC in GYP broth (2.0 mg/ml). Moreover, a large concentration of salts can also affect lactoferrin structure. Lactoferrin has two lobes, N and C, and each of them can be attached to a metal atom, such as iron (Fe^{2+} and Fe^{3+}), copper (Cu^{2+}), zinc (Zn^{2+}) or manganese (Mn^{2+}) (EL-Fakharany, 2020). This binding may compromise its antimicrobial activity due to a new three-dimensional conformation acquired by the molecule (Alhalwani et al., 2020). Apo-lactoferrin (free lactoferrin) has an open conformation, while its holo form (linked to iron) has a more closed structure (Fernández-Menéndez et al., 2020). The structure of apo-lactoferrin consists of two globular lobes (lobes N and C) connected by a three-turn alpha helix. Each lobe forms a slit with great affinity for the Fe^{3+} ion in the presence of a carbonate anion (EL-Fakharany, 2020).

Therefore, in mediums with a high concentration of iron or zinc, as present in the TSB culture medium (Table 6), lactoferrin's antimicrobial capacity is affected due to the modification of its spatial conformation, which affects the availability of its positive active sites, reducing its interaction with the microorganism's anionic sites.

Moreover, as the ionic strength of the solutions increases, the magnitude of the zeta potential of nanoparticles usually decreases and tends to zero due to screening effects (Bhattacharjee, 2016). This shielding of loads can cause agglomeration of nanoparticles and instability with a consecutive drop in nanoparticle functionality (Feng et al., 2020). It is worth mentioning that the reduction in bacteriostatic effects was more intense for nanoparticles than pure lactoferrin. For nanoparticles, the presence of high salt concentrations led to the absence of bacteriostatic action, while in the case of pure lactoferrin only an increase in MIC was observed (Table 5).

This is probably related to the lower flexibility of lactoferrin when complexed to gellan gum as previously reported for the complexation of other polymers (Skolnick and Fixman, 1977). The decrease in lactoferrin flexibility can reduce its interaction with the bacterial membrane and, consequently, inhibit bacteriostatic effects.

The tests for minimum bactericidal concentration showed the growth of microorganisms for all samples (Table 5), indicating the absence of bactericidal action for nanoparticles and pure compounds.

4.2. Action of nanoparticles on strawberry coatings

4.2.1. Appearance of strawberries during storage

Fig. 5 shows the visual appearance of the control and treated strawberries over time.

The control group showed an expressive size shrinkage over time, reflecting the intense weight loss of the strawberries. Conversely, the samples with the CMC coating showed fewer changes in size during storage, which indicates that CMC was a good barrier to the moisture loss of the samples.

In all strawberries, the color gradually became darker due to the loss of mass and lower production of anthocyanins (Martinsen et al., 2020). In the control group and in strawberries treated only with nanoparticles (in the absence of CMC) the fruit epidermis wrinkled and withered after 120 h. Moreover, the control group had some visible mold growth points at the end of storage time, which was not observed in the presence of nanoparticles. These observations indicate that the nanoparticles alone were not efficient in maintaining the visual aspect of strawberries, but
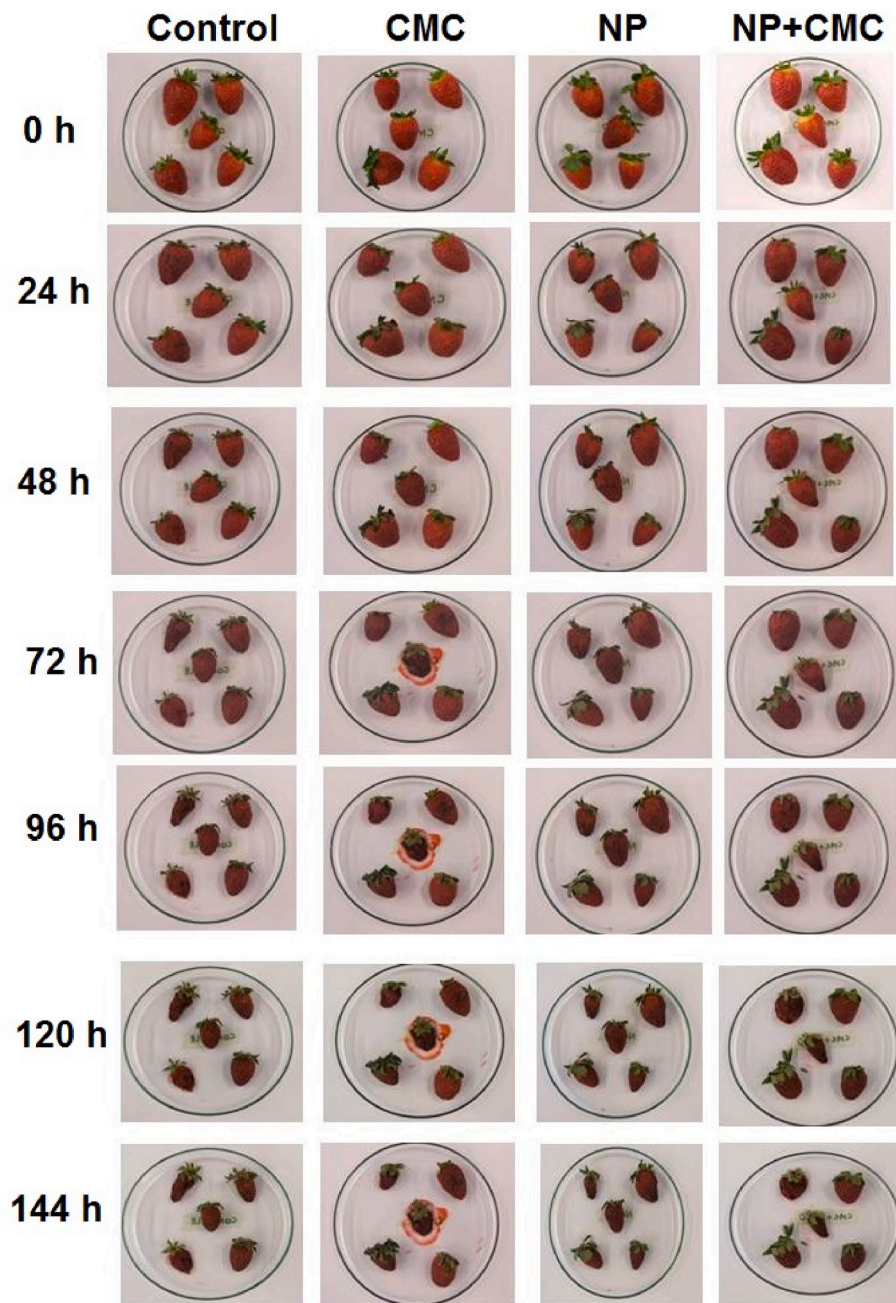
Fig. 5. Appearance of strawberries without coating (control), coated with carboxymethylcellulose (CMC), 9L:1G nanoparticles (NP) and 9L:1G nanoparticles plus carboxymethylcellulose (NP + CMC).

were efficient in reducing the size and color modifications in the presence of CMC during storage.

4.2.2. Weight loss, TA, TSS and pH

The weight loss of postharvest strawberries is related to the loss of moisture, carbon reserves or water by transpiration due to the respiration that occurs in the fruit epidermis and its stomata (Vogler and Ernst, 1999). All groups evaluated showed an increasing tendency to lose weight over the storage period (Fig. 6). However, the weight loss of fresh strawberries (control) was greater than those of other treatments.

A lower weight variation was observed for strawberries treated with CMC and nanoparticles plus CMC. These coatings acted as barriers to gas exchange and probably reduced the transpiration rate of the fruits (Gao et al., 2020). They can also have reduced the fruit's oxygen consumption

and respiration rate, resulting in less weight loss for these strawberries (Arowora et al., 2013).

In fact, the values of titratable acidity (TA), the content of total soluble solids over time (TSS) and the pH of the samples indicate (Table 7) that these samples present a lower maturation rate over time.

TSS has a close relationship with fruit maturity, respiratory rate and water loss (Gao et al., 2020; Sogvar et al., 2016a). All groups exhibited increasing TSS values over time due to the usual sucrose synthesis in the maturation process. The highest TSS values were observed in the control group and in strawberries treated with only nanoparticles, which also showed greater water loss (Fig. 6).

Strawberries coated with CMC and CMC + nanoparticles showed lower soluble solids values at the end of storage, probably due to the lower rate of respiration and metabolic activity of the fruits, related to
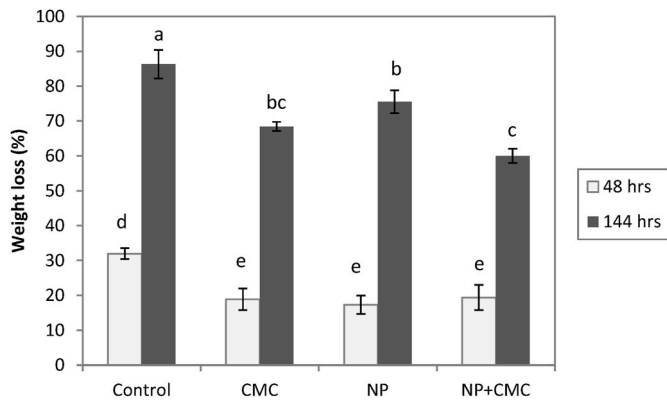
Fig. 6. Weight loss of strawberry during storage. Different letters indicate significant differences (p-value < 0.05).

Table 7
Titratable acidity (TA), total soluble solids (TSS) content and pH of strawberries over time.

Analyses	Storage time (hours)	Control	CMC	NP	NP + CMC
TA (%)	0	0.158 ± 0.001^{Aa}	0.158 ± 0.001^{Aa}	0.158 ± 0.001^{Aa}	0.158 ± 0.001^{Aa}
	48	0.142 ± 0.002^{Ab}	0.122 ± 0.003^{Bb}	0.125 ± 0.001^{Bb}	0.125 ± 0.002^{Bb}
	144	0.107 ± 0.003^{Ac}	0.110 ± 0.001^{ABc}	0.106 ± 0.003^{Ac}	0.116 ± 0.001^{Bc}
TSS (%)	0	6.80 ± 0.20^{Aa}	6.80 ± 0.20^{Aa}	6.80 ± 0.20^{Aa}	6.80 ± 0.20^{Aa}
	48	8.20 ± 0.26^{Ab}	8.90 ± 0.10^{Ab}	8.70 ± 0.35^{Ab}	8.40 ± 0.53^{Ab}
	144	16.37 ± 0.15^{Ac}	14.10 ± 0.52^{Bc}	15.23 ± 0.25^{Cc}	13.10 ± 0.10^{Dc}
pH	0	3.29 ± 0.04^{Aa}	3.29 ± 0.04^{Aa}	3.29 ± 0.04^{Aa}	3.29 ± 0.04^{Aa}
	48	3.33 ± 0.04^{Aa}	3.34 ± 0.02^{Aa}	3.17 ± 0.03^{Ba}	3.18 ± 0.03^{Bb}
	144	3.61 ± 0.05^{Ab}	3.52 ± 0.09^{ABb}	3.58 ± 0.11^{Ab}	3.41 ± 0.02^{Bc}

Means followed by different uppercase letters on the same line indicate significant differences (p-value <0.05). Different lowercase letters on the same column indicate significant differences between means over time (p-value <0.05).

the reduction in the conversion of sugar into CO_2 and water, caused by the modification of the internal atmosphere with the coating (Ghasemnezhad et al., 2011).

The main components of titratable acidity are organic acids, which are substrates for enzymatic reactions related to respiration (Hazrati et al., 2017). Titratable acidity reflects a change in the percentage of citric acid in fresh fruits and is one of the main acids of strawberries (Abu Salha and Gedanken, 2021). In general, TA values tend to decrease for all samples over time. However, this drop was less intense for strawberries coated with CMC + nanoparticles.

The pH is known to reflect changes in the organic acid content of fresh fruits during storage (Jiang et al., 2020). The pH values of all treatments increased during storage, as the acid content of the fruit decreased during ripening and as the fruits used organic acids in the respiratory process (Echeverria and Valich, 1989; Al-Asmar et al., 2020).

4.2.3. Total aerobic mesophilic bacteria counts
The initial populations of mesophilic bacteria were 2.95 Log CFU/ml and increased during storage for the control and treated fruits (Fig. 7). Overall, the coating with CMC did not directly affect mesophilic growth after 48h of storage in comparison with the control, but led to a decrease in microorganism counts after 144h. Most likely, the inhibition of
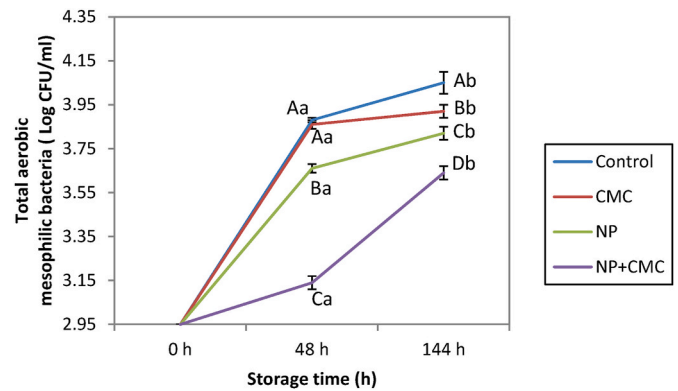

Fig. 7. Total counts of aerobic mesophilic bacteria (log CFU/ml) in strawberries submitted to different treatments during storage time at 25 °C and 50% RH. Different uppercase letters indicate significant differences between treatments (p-value <0.05). Different lowercase letters indicate significant differences between means over time (p-value <0.05).

physicochemical deterioration over time due to CMC presence, as observed in the pH, TA and TSS analyses (Table 7), helped to retard bacterial growth.

The nanoparticles were capable of inhibiting mesophilic bacterial growth over time in relation to the control samples. However, this behavior was even more intense in the presence of CMC + nanoparticles. In addition to the CMC contribution to retard physicochemical alterations on strawberries over time, it probably helped the nanoparticles adhere to the fruit surface, which resulted in a more intense bacteriostatic effect.

5. Conclusion

The tests of antimicrobial action demonstrated that the surface charge and size are fundamental parameters for the effectiveness of nanoparticles against the evaluated bacteria. The 9L:1G ratio showed greater zeta potential and smaller hydrodynamic size compared to the other particles, being the only sample to have bacteriostatic action. The medium was also shown to be relevant to lactoferrin antimicrobial activity. The presence of large amounts of divalent cations in the TSB broth inhibited the antimicrobial potential of lactoferrin due to the competition of salts for the anionic sites of the microorganism membrane, screening of nanoparticle charges. The nanosize of particles resulted in an intensification of antimicrobial activity of lactoferrin with respect to the pure protein, as the MIC dropped from 2 mg/ml for pure lactoferrin to 0.3 mg/ml for nanoparticle 9L:1G. Lactoferrin-gellan gum complexation was successful in intensifying the antimicrobial properties of lactoferrin.

The nanoparticle application on the strawberry coating reduced the weight loss and growth of mesophilic bacteria during storage. These results along with the decrease in the physicochemical changes of strawberries during storage, prove that the nanoparticles were effective in preserving and extending the shelf life of the fruits. Nevertheless, further research addressing the improvement of strawberries visual appearance during storage would be fruitful.

CRediT authorship contribution statement

Larissa G.R. Duarte: Investigation, Formal analysis, Writing – original draft, Data curation, Visualization. **William M.P. Alencar:** Methodology, Formal analysis, Visualization. **Raiza Iacuzio:** Investigation. **Nathália C.C. Silva:** Resources, Supervision, Methodology. **Carolina S.F. Picone:** Conceptualization, Resources, Supervision, Writing – review & editing, Project administration, Funding acquisition.

Declaration of competing interest

The authors declare that they have no known competing financial interests or personal relationships that could have appeared to influence the work reported in this paper.

Acknowledgments

References

Abu Salha, B., Gedanken, A., 2021. Extending the shelf life of strawberries by the sonochemical coating of their surface with nanoparticles of an edible anti-bacterial compound. Appl. Nanosci. 2 (1), 14–24. https://doi.org/10.3390/applnano2010002.

Agibayeva, L.E., Kaldybekov, D.B., Porfiryeva, N.N., Garipova, V.R., Mangazbayeva, R. A., Moustafine, R.I., Semina, I.I., Mun, G.A., Kudaibergenov, S.E., Khutoryanskiy, V. V., 2020. Gellan gum and its methacrylated derivatives as in situ gelling mucoadhesive formulations of pilocarpine: in vitro and in vivo studies. Int. J. Pharm. 577, 119093 https://doi.org/10.1016/j.ijpharm.2020.119093.

Al-Asmar, A., Giosafatto, C.V.L., Sabbah, M., Sanchez, A., Villalonga Santana, R., Mariniello, L., 2020. Effect of mesoporous silica nanoparticles on the physicochemical properties of pectin packaging material for strawberry wrapping. Nanomaterials 10 (1), 52. https://doi.org/10.3390/nano10010052.

Alhalwani, Amani Y., Davey, Rachel L., Kaul, Navneeta, Barbee, Scott A., Huffman, J. Alex, 2020. Modification of lactoferrin by peroxynitrite reduces its antibacterial activity and changes protein structure. Protein Struct. Funct. Bioinf. 88 (1), 166–174. https://doi.org/10.1002/prot.25782.

Arowora, K.A., Williams, J.O., Adetunji, C.O., Fawole, O.B., Afolayan, S.S., Olaleye, O.O., Ogundele, B.A., 2013. Effects of Aloe vera coatings on quality characteristics of oranges stored under cold storage. Greener .J. Agric. Sci. 3 (1), 39–47. https://doi.org/10.15580/GJAS.2013.1.110112192.

Babaei, J., Khodaiyan, F., Mohammadian, M., 2019. Effects of enriching with gellan gum on the structural, functional, and degradation properties of egg white heat-induced hydrogels. Int. J. Biol. Macromol. 128, 94–100. https://doi.org/10.1016/j.ijbiomac.2019.01.116.

Baker, E.N., Baker, H.M., 2005. Molecular structure, binding properties and dynamics of lactoferrin. Cell. Mol. Life Sci. 62, 2531–2539. https://doi.org/10.1007/s00018-005-5368-9.

Barreiras, D.G., Ruiz, F.M., Gomes, J.E.G., Souza, B.M.S., 2020. Eficácia da ação antimicrobiana do extrato de própolis de abelha jataí (*Tetragonisca angustula*) em bactérias Gram-positivas e Gram-negativas. Caderno De Ciências Agrárias 12, 1–5. https://doi.org/10.35699/2447-6218.2020.15939.

Bastos, A.R., da Silva, L.P., Maia, F.R., Pina, S., Rodrigues, T., Sousa, F., Reis, R.L., 2019. Lactoferrin-hydroxyapatite containing spongy-like hydrogels for bone tissue engineering. Materials 12 (13), 2074. https://doi.org/10.3390/ma12132074.

Bellamy, W., Takase, M., Yamauchi, K., Wakabayashi, H., Kawase, K., Tomita, M., 1992. Identification of the bactericidal domain of lactoferrin. Biochim. Biophys. Acta 1121, 130–136. https://doi.org/10.1016/0167-4838(92)90346-F.

Bengoechea, C., Peinado, I., McClements, D.J., 2011. Formation of protein nanoparticles by controlled heat treatment of lactoferrin: factors affecting particle characteristics. Food Hydrocolloids 25 (5), 1354–1360. https://doi.org/10.1016/j.foodhyd.2010.12.014.

Bhattacharjee, S., 2016. DLS and zeta potential – what they are and what they are not? J. Contr. Release 235, 337–351. https://doi.org/10.1016/j.jconrel.2016.06.017.

Bokkhim, H., Bansal, N., Grøndahl, L., Bhandari, B., 2015. In-vitro digestion of different forms of bovine lactoferrin encapsulated in alginate micro-gel particles. Food Hydrocolloids 52, 231–242. https://doi.org/10.1016/j.foodhyd.2015.07.007.

Bollimpelli, V.S., Kumar, P., Kumari, S., Kondapi, A.K., 2016. Neuroprotective effect of curcumin-loaded lactoferrin nanoparticles against rotenone induced neurotoxicity. Neurochem. Int. 95, 37–45. https://doi.org/10.1016/j.neuint.2016.01.006.

Bourbon, A.I., Cerqueira, M.A., Vicente, A.A., 2016. Encapsulation and controlled release of bioactive compounds in lactoferrin-glycomacropeptide nanohydrogels: curcumin and caffeine as model compounds. J. Food Eng. 180, 110–119. https://doi.org/10.1016/j.jfoodeng.2016.02.016.

Bourbon, A.I., Martins, J.T., Pinheiro, A.C., Madalena, D.A., Marques, A., Nunes, R., Vicente, A.A., 2019. Nanoparticles of lactoferrin for encapsulation of food ingredients. In: Biopolymer Nanostructures for Food Encapsulation. Academic Press, pp. 147–168.

Cassanelli, M., Prosapio, V., Norton, I., Mills, T., 2019. Role of the drying technique on the low-acyl gellan gum gel structure: molecular and macroscopic investigations. Food Bioprocess Technol. 12 (2), 313–324. https://doi.org/10.1007/s11947-018-2210-6.

Chandrasekaran, R., Millane, R.P., Arnott, S., Atkins, E.D.T., 1988. The crystal structure of gellan. Carbohydr. Res. 175 (1), 1–15. https://doi.org/10.1016/0008-6215(88)80151-4.

Chen, Y., Zhao, Z., Xia, G., Xue, F., Chen, C., Zhang, Y., 2020. Fabrication and characterization of zein/lactoferrin composite nanoparticles for encapsulating 7, 8-dihydroxyflavone: enhancement of stability, water solubility and bioaccessibility. Int. J. Biol. Macromol. 146, 179–192. https://doi.org/10.1016/j.ijbiomac.2019.12.251.

de Jong, S., van de Velde, F., 2007. Charge density of polysaccharide controls microstructure and large deformation properties of mixed gels. Food Hydrocolloids 21 (7), 1172–1187. https://doi.org/10.1016/j.foodhyd.2006.09.004.

Duca, G., Anghel, L., Erhan, R.V., 2018. Structural aspects of lactoferrin and serum transferrin observed by ftir spectroscopy. Chem.J.Moldova.Gen.Ind.Ecol.Chem 13 (1), 2345. https://doi.org/10.19261/cjm.2018.482, 1688.

Echeverria, E., Valich, J., 1989. Enzymes of sugar and acid metabolism in stored 'Valencia' oranges. J. Am. Soc. Hortic. Sci. 114 (3), 445–449.

EL-Fakharany, E.M., 2020. Nanoformulation of lactoferrin potentiates its activity and enhances novel biotechnological applications. Int. J. Biol. Macromol. 165, 970–984. https://doi.org/10.1016/j.ijbiomac.2020.09.235.

Elbarbary, H.A., Abdou, A.M., Park, E.Y., Nakamura, Y., Mohamed, H.A., Sato, K., 2010. Novel antibacterial lactoferrin peptides generated by rennet digestion and autofocusing technique. Int. Dairy J. 20 (9), 646–651. https://doi.org/10.1016/j.idairyj.2009.12.019.

Fasolin, L.H., Picone, C.S.F., Santana, R.C., Cunha, R.L., 2013. Production of hybrid gels from polysorbate and gellan gum. Food Res. Int. 54 (1), 501–507. https://doi.org/10.1016/j.foodres.2013.07.026.

Feng, Y., Kilker, S.R., Lee, Y., 2020. Surface charge (zeta-potential) of nanoencapsulated food ingredients. In: Characterization of Nanoencapsulated Food Ingredients. Academic Press, pp. 213–241.

Fernández, P.L., 2015. Velázquez, farmacología básica y clínica. panamericana. In: Médica Panamericana (eBook online).

Fernández-Menéndez, S., Peixoto, R.R., Fernandez-Colomer, B., Suarez-Rodriguez, M., Sanz-Medel, A., Fernandez-Sanchez, M.L., 2020. Effect of holder pasteurisation on total concentrations and iron-binding profiles of holo-lactoferrin used as fortifier in donor human milk. Int. Dairy J. 100, 104564 https://doi.org/10.1016/j.idairyj.2019.104564.

Ferreira, D.F., 2019. Sisvar: a computer analysis system to fixed effects split plot type designs. Revista Brasileira de Biometria 37 (4), 529–535. https://doi.org/10.28951/rbb.v37i4.450.

Franco, I., Perez, M.D., Conesa, C., Calvo, M., Sanchez, L., 2018. Effect of technological treatments on bovine lactoferrin: an overview. Food Res. Int. 106, 173–182. https://doi.org/10.1016/j.foodres.2017.12.016.

Gao, Y., Xu, D., Ren, D., Zeng, K., Wu, X., 2020. Green synthesis of zinc oxide nanoparticles using Citrus sinensis peel extract and application to strawberry preservation: a comparison study. LWT - Food Sci. Technol. (Lebensmittel-Wissenschaft -Technol.) 126, 109297. https://doi.org/10.1016/j.lwt.2020.109297.

Ghasemnezhad, M., Nezhad, M.A., Gerailoo, S., 2011. Changes in postharvest quality of loquat (Eriobotrya japonica) fruits influenced by chitosan. Hortic.Environ. Biotechnol. 52 (1), 40–45. https://doi.org/10.1007/s13580-011-0028-5.

Gonzalez-Chavez, S.A., Arevalo-Gallegos, S., Rascon-Cruz, Q., 2009. Lactoferrin: structure, function and applications. Int. J. Antimicrob. Agents 33 (4), 301. https://doi.org/10.1016/j.ijantimicag.2008.07.020 e1.

Grasdalen, H., Smidsrød, O., 1987. Gelation of gellan gum. Carbohydr. Polym. 7 (5), 371–393. https://doi.org/10.1016/0144-8617(87)90004-X.

Gulão, E.D.S., de Souza, C.J., da Silva, F.A., Coimbra, J.S., Garcia-Rojas, E.E., 2014. Complex coacervates obtained from lactoferrin and gum Arabic: formation and characterization. Food Res. Int. 65, 367–374. https://doi.org/10.1016/j.foodres.2014.08.024.

Haney, E.F., Lau, F., Vogel, H.J., 2007. Solution structures and model membrane interactions of lactoferrampin, an antimicrobial peptide derived from bovine lactoferrin. Biochim. Biophys. Acta Biomembr. 1768 (10), 2355–2364. https://doi.org/10.1016/j.bbamem.2007.04.018.

Hazrati, S., Kashkooli, A.B., Habibzadeh, F., Tahmasebi-Sarvestani, Z., Sadeghi, A.R., 2017. Evaluation of aloe vera gel as an alternative edible coating for peach fruits during cold storage period. Gesunde Pflanz. 69 (3), 131–137. https://doi.org/10.1007/s10343-017-0397-5.

Holler, J.F., Skoog, D.A., Crouch, S.R., 2009. Princípios de análise instrumental. Bookman.

Horinaka, J., Kani, K., Hori, Y., Maeda, S., 2004. Effect of pH on the conformation of gellan chains in aqueous systems. Biophys. Chem. 111 (3), 223–227. https://doi.org/10.1016/j.bpc.2004.06.003.

Ibrahim Al-Mashahedah, A.M., Kanwar, R.K., Kanwar, J.R., 2019. Utility of nanomedicine targeting scar-forming myofibroblasts to attenuate corneal scarring and haze. Nanomedicine 14 (8), 1049–1072. https://doi.org/10.2217/nnm-2017-0305.

Iglesias-Figueroa, B.F., Espinoza-Sánchez, E.A., Siqueiros-Cendón, T.S., Rascón- Cruz, Q., 2019. Lactoferrin as a nutraceutical protein from milk, an overview. Int. Dairy J. 89, 37–41. https://doi.org/10.1016/j.idairyj.2018.09.004.

Iucci, L., Patrignani, F., Vallicelli, M., Guerzoni, M.E., Lanciotti, R., 2007. Effects of high pressure homogenization on the activity of lysozyme and lactoferrin against Listeria

monocytogenes. Food Control 18 (5), 558–565. https://doi.org/10.1016/j.foodcont.2006.01.005.

Jiang, Y., Yu, L., Hu, Y., Zhu, Z., Zhuang, C., Zhao, Y., Zhong, Y., 2020. The preservation performance of chitosan coating with different molecular weight on strawberry using electrostatic spraying technique. Int. J. Biol. Macromol. 151, 278–285. https://doi.org/10.1016/j.ijbiomac.2020.02.169.

Kanwar, J.R., Roy, K., Patel, Y., Zhou, S.-F., Singh, M.R., Singh, D., 2015. Multifunctional iron bound lactoferrin and nanomedicinal approaches to enhance its bioactive functions. Molecules 20, 9703–9731. https://doi.org/10.3390/molecules20069703.

Kumar, P., Lakshmi, Y.S., Kondapi, A.K., 2017. An oral formulation of efavirenz-loaded lactoferrin nanoparticles with improved biodistribution and pharmacokinetic profile. HIV Med. 18 (7), 452–462. https://doi.org/10.1111/hiv.12475.

Lam, S.J., Wong, E.H.H., Boyer, C., Qiao, G.G., 2018. Antimicrobial polymeric nanoparticles. Prog. Polym. Sci. 76, 40–64. https://doi.org/10.1016/j.progpolymsci.2017.07.007.

Liu, W., Kong, Y., Tu, P., Lu, J., Liu, C., Liu, W., 2017. Physical-chemical stability and in vitro digestibility of hybrid nanoparticles based on the layer-by-layer assembly of lactoferrin and BSA on liposomes. Food Funct. 8 (4), 1688–1697. https://doi.org/10.1039/C7FO00308K.

Martinsen, B.K., Aaby, K., Skrede, G., 2020. Effect of temperature on stability of anthocyanins, ascorbic acid and color in strawberry and raspberry jams. Food Chem. 316, 126297. https://doi.org/10.1016/j.foodchem.2020.126297.

McCarthy, N.A., Kelly, A.L., O'Mahony, J.A., Fenelon, M.A., 2014. Sensitivity of emulsions stabilised by bovine β-casein and lactoferrin to heat and CaCl2. Food Hydrocolloids 35, 420–428. https://doi.org/10.1016/j.foodhyd.2013.06.021.

Mirón-Mérida, V.A., Yáñez-Fernándezb, J., Montañez-Barragána, B., Barragán Huerta, B. E., 2019. Valorization of coffee parchment waste (Coffea arabica) as a source of caffeine and phenolic compounds in antifungal gellan gum films. LWT - Food Sci. Technol. (Lebensmittel-Wissenschaft -Technol.) 101, 167–174. https://doi.org/10.1016/j.lwt.2018.11.013.

Moore, S.A., Anderson, B.F., Groom, C.R., Haridas, M., Baker, E.N., 1997. Three-dimensional structure of diferric bovine lactoferrin at 2.8 A resolution. J. Mol. Biol. 274 (2), 222–236. https://doi.org/10.1006/jmbi.1997.1386.

Nakamura, K., 2002. Potent antimicrobial effects of the glycosylated lactoferrin. Food. Preservation Sci. 28 (5), 243–246. https://doi.org/10.5891/jafps.28.243.

Oliveira, D.R.B., Michelon, M., de Figueiredo Furtado, G., Sinigaglia-Coimbra, R., Cunha, R.L., 2016. β-Carotene-loaded nanostructured lipid carriers produced by solvent displacement method. Food Res. Int. 90, 139–146. https://doi.org/10.1016/j.foodres.2016.10.038.

O'Neill, M.A., Silvendran, R.R., Morris, J., 1983. Structure of the acidic extracelular gelling polysaccharide produced by Pseudomonas elodea. Carbohydr. Res. 124 (1), 123–133. https://doi.org/10.1016/0008-6215(83)88360-8.

Padrão, J., Ribeiro, S., Lanceros-Méndez, S., Rodrigues, L.R., Dourado, F., 2020. Effect of bacterial nanocellulose binding on the bactericidal activity of bovine lactoferrin. Heliyon 6 (7), e04372. https://doi.org/10.1016/j.heliyon.2020.e04372.

Pan, Y., Shiell, B., Wan, J., Coventry, M.J., Roginski, H., Lee, A., Michalski, W.P., 2007. The molecular characterisation and antimicrobial activity of amidated bovine lactoferrin. Int. Dairy J. 17 (6), 606–616. https://doi.org/10.1016/j.idairyj.2006.08.005.

Peinado, I., Lesmes, U., Andrés, A., McClements, J.D., 2010. Fabrication and morphological characterization of biopolymer particles formed by electrostatic complexation of heat treated lactoferrin and anionic polysaccharides. Langmuir 26 (12), 9827–9834. https://doi.org/10.1021/la1001013.

Picone, C.S.F., Cunha, R.L., 2013. Chitosan–gellan electrostatic complexes: influence of preparation conditions and surfactant presence. Carbohydr. Polym. 94.

Quintieri, L., Caputo, L., Monaci, L., Deserio, D., Morea, M., Baruzzi, F., 2012. Antimicrobial efficacy of pepsin-digested bovine lactoferrin on spoilage bacteria contaminating traditional Mozzarella cheese. Food Microbiol. 31 (1), 64–71. https://doi.org/10.1016/j.fm.2012.02.015.

Ren, W., Cheng, W., Wang, G., Liu, Y., 2017. Developments in antimicrobial polymers. J. Polym. Sci. Polym. Chem. 55 (4), 632–639. https://doi.org/10.1002/pola.28446.

Ribas Fonseca, L., Porto Santos, T., Czaikoski, A., Lopes Cunha, R., 2020. Modulating properties of polysaccharides nanocomplexes from enzymatic hydrolysis of chitosan. Food Res. Int. 137, 109642. https://doi.org/10.1016/j.foodres.2020.109642.

Sabra, S., Agwa, M.M., 2020. Lactoferrin, a unique molecule with diverse therapeutical and nanotechnological applications. Int. J. Biol. Macromol. 164, 1046–1060. https://doi.org/10.1016/j.ijbiomac.2020.07.167.

Santos, M.B., da Costa, A.R., Garcia-Rojas, E.E., 2018. Heteroprotein complex coacervates of ovalbumin and lysozyme: formation and thermodynamic characterization. Int. J. Biol. Macromol. 106, 1323–1329. https://doi.org/10.1016/j.ijbiomac.2017.08.132.

Saraiva, C.S., Coimbra, J.S.R., Teixeira, A.V.N.C., Oliveira, E.B., Teofilo, R.F., Costa, A.R., Barbosa, E.A.A., 2017. Formation and characterization of supramolecular structures of β-lactoglobulin and lactoferrin proteins. Food Res. Int. 100, 674–681. https://doi.org/10.1016/j.foodres.2017.07.065.

Schmitt, C., Sanchez, C., Desobry-Banon, S., Hardy, J., 1998. Structure and technofunctional properties of protein-polysaccharide complexes: a review. Crit. Rev. Food Sci. Nutr. 38 (8), 689–753. https://doi.org/10.1080/10408699891274354.

Seibert, J.B., Bautista-Silva, J.P., Amparo, T.R., Petit, A., Pervier, P., Almeida, J.C.S., Azevedo, M.C., Silveira, B.M., Brandão, G.C., Souza, G.H.B., Teixeira, L.F.M., Santos, O.D.H., 2019. Development of propolis nanoemulsion with antioxidant and antimicrobial activity for use as a potential natural preservative. Food Chem. 287, 61–67. https://doi.org/10.1016/j.foodchem.2019.02.078.

Shahidi, F., Roshanak, S., Javadmanesh, A., Yazdi, F.T., Pirkhezranian, Z., Azghandi, M., 2020. Evaluation of antimicrobial properties of bovine lactoferrin against foodborne

pathogenic microorganisms in planktonic and biofilm forms (in vitro). J.Consum. Protect.Food Saf. 15 (3), 277–283. https://doi.org/10.1007/s00003-020-01280-3.

Skolnick, J., Fixman, M., 1977. Electrostatic persistence length of a wormlike polyelectrolyte. Macromolecules 10 (5), 944–948. https://doi.org/10.1021/ma60059a011.

Sogvar, O.B., Koushesh Saba, M., Emamifar, A., 2016a. Aloe vera and ascorbic acid coatings maintain postharvest quality and reduce microbial load of strawberry fruit. Postharvest Biol. Technol. 114, 29–35. https://doi.org/10.1016/j.postharvbio.2015.11.019.

Sogvar, O.B., Saba, M.K., Emamifar, A., Hallaj, R., 2016b. Influence of nano-ZnO on microbial growth, bioactive content and postharvest quality of strawberries during storage. Innovat. Food Sci. Emerg. Technol. 35, 168–176. https://doi.org/10.1016/j.ifset.2016.05.005.

Su, H., Xu, Y., 2018. Application of ITC-based characterization of thermodynamic and kinetic association of ligands with proteins in drug design. Front. Pharmacol. 9, 1133. https://doi.org/10.3389/fphar.2018.01133.

Sworn, G., Kasapis, S., 1998. Effect of conformation and molecular weight of co-solute on the mechanical properties of gellan gum gels. Food Hydrocolloids 12 (3), 283–290. https://doi.org/10.1016/S0268-005X(98)00016-2.

Tammam, S.N., Azzazy, H.M., Lamprecht, A., 2018. Nuclear and cytoplasmic delivery of lactoferrin in glioma using chitosan nanoparticles: cellular location dependent-action of lactoferrin. Eur. J. Pharm. Biopharm. 129, 74–79. https://doi.org/10.1016/j.ejpb.2018.05.027.

Tkaczewska, J., 2020. Peptides and protein hydrolysates as food preservatives and bioactive components of edible films and coatings-A review. Trends Food Sci. Technol. 106, 298–311. https://doi.org/10.1016/j.tifs.2020.10.022.

Tomita, S., Shirasaki, N., Matsuyama, J., Benno, Y., Kiyosawa, I., 2006. Growth behavior of Clostridium perfringens cells aggregated by bovine lactoferrin in the presence of lipoteichoic acid. Food.Preservation Sci. 32 (3), 85–89. https://doi.org/10.5891/jafps.32.3_85.

Torres, O., Yamada, A., Rigby, N.M., Hanawa, T., Kawano, Y., Sarkar, A., 2019. Gellan gum: a new member in the dysphagia thickener family. Biotribology 17, 8–18. https://doi.org/10.1016/j.biotri.2019.02.002.

Turgeon, S.L., Laneuville, S.I., 2009. Protein polysaccharide coacervates and complexes. In: Modern Biopolymer Science. Academic Press, pp. 327–363.

Ueno, H.M., Ueda, N., Morita, M., Kakehi, Y., Kobayashi, T., 2012. Thermal stability of the iron–lactoferrin complex in aqueous solution is improved by soluble soybean polysaccharide. Food Biophys. 7 (3), 183–189. https://doi.org/10.1007/s11483-012-9256-1.

Vega Chaparro, S.C., Valencia Salguero, J.T., Martínez Baquero, D.A., Rosas Pérez, J.E., 2018. Effect of Polyvalence on the Antibacterial Activity of a Synthetic Peptide Derived from Bovine Lactoferricin against Healthcare-Associated Infectious Pathogens. BioMed research international. https://doi.org/10.1155/2018/5252891, 2018.

Vieira, D.D.S., Polveiro, R.C., Butler, T.J., Hackett, T.A., Braga, C.P., Puniya, B.L., Feitosa, F.L., 2021. An in silico, structural, and biological analysis of lactoferrin of different mammals. Int. J. Biol. Macromol. 187, 119–126. https://doi.org/10.1016/j.ijbiomac.2021.07.102.

Vogler, B.K., Ernst, E., 1999. Aloe vera: a systematic review of its clinical effectiveness. Br. J. Gen. Pract. 49 (447), 823–828.

Wang, Y., Pillai, P.K.S., Nickerson, M.T., 2019. Effect of molecular mass and degree of substitution of carboxymethyl cellulose on the formation electrostatic complexes with lentil protein isolate. Food Res. Int. 126, 108652 https://doi.org/10.1016/j.foodres.2019.108652.

Wang, Y., Morton, J.D., Bekhit, A.E.D.A., Carne, A., Mason, S.L., 2021. Amino acid sequences of lactoferrin from red deer (Cervus elaphus) milk and antimicrobial activity of its derived peptides lactoferricin and lactoferrampin. Foods 10 (6), 1305. https://doi.org/10.3390/foods10061305.

Xia, Z., Villarreal, E., Wang, H., Lau, B.L., 2020. Nanoscale surface curvature modulates nanoparticle-protein interactions. Colloids Surf. B Biointerfaces 190, 110960. https://doi.org/10.1016/j.colsurfb.2020.110960.

Xiong, W., Ren, C., Tian, M., Yang, X., Li, J., Li, B., 2017. Complex coacervation of ovalbumin-carboxymethylcellulose assessed by isothermal titration calorimeter and rheology: effect of ionic strength and charge density of polysaccharide. Food Hydrocolloids 73, 41–50. https://doi.org/10.1016/j.foodhyd.2017.06.031.

Xu, X.-J., Fang, S., Li, Y.-H., Zhang, F., Shao, Z.-P., Zeng, Y.-T., Chen, J., Meng, Y.-C., 2019. Effects of low acyl and high acyl gellan gum on the thermal stability of purple sweet potato anthocyanins in the presence of ascorbic acid. Food Hydrocolloids 86, 116–123. https://doi.org/10.1016/j.foodhyd.2018.03.007.

Yang, S., Dai, L., Mao, L., Liu, J., Yuan, F., Li, Z., Gao, Y., 2019. Effect of sodium tripolyphosphate incorporation on physical, structural, morphological and stability characteristics of zein and gliadin nanoparticles. Int. J. Biol. Macromol. 136, 653–660. https://doi.org/10.1016/j.ijbiomac.2019.06.052.

Yang, W., Deng, C., Xu, L., Jin, W., Zeng, J., Li, B., Gao, Y., 2020. Protein-neutral polysaccharide nano- and micro-biopolymer complexes fabricated by lactoferrin and oat β-glucan: structural characteristics and molecular interaction mechanisms. Food Res. Int. 132, 109111 https://doi.org/10.1016/j.foodres.2020.109111.

Zhang, J.L., Di, W., Gong, P.M., Lin, K., Lyu, L.Z., Zhang, L.W., Ma, Y., 2019. Direct and fast capture lactoferrin from cheese whey on nanoparticles of Fe3O4 combined with concanavalin A. Food Chem. 274, 314–318. https://doi.org/10.1016/j.foodchem.2018.08.115.

Zheng, J., Gao, Q., Tang, C., Ge, G., Zhao, M., Sun, W., 2020. Heteroprotein complex formation of soy protein isolate and lactoferrin: thermodynamic formation mechanism and morphologic structure. Food Hydrocolloids 100, 105415. https://doi.org/10.1016/j.foodhyd.2019.105415.